WNT3A-loaded exosomes enable cartilage repair

Bethan L. Thomas[1*], Suzanne E. Eldridge[1*], Babak Nosrati[4], Mario Alvarez[1], Anne-Sophie Thorup[1], Giovanna Nalesso[3], Sara Caxaria[1], Aida Barawi[1], James G. Nicholson[1], Mauro Perretti[1], Carles Gaston-Massuet[1], Costantino Pitzalis[1], Alison Maloney[2], Adrian Moore[2], Ray Jupp[2], and Francesco Dell'Accio[1].

[1]Barts and the London School of Medicine and Dentistry, William Harvey Research Institute, Queen Mary University of London, London, EC1M 6BQ, UK.

[2]UCB Pharma, Slough, Berkshire, SL1 3WE, UK.

[3]School of Veterinary Medicine, University of Surrey, Daphne Jackson Road, Guildford, GU2 7AL, UK.

[4]Dipartimento di scienza e tecnologia del farmaco, Università degli Studi di Torino, 10125 Torino, Italy.

*Co-first authours

Corresponding Authors:
Dr. Bethan Lynne Thomas
b.l.thomas@qmul.ac.uk
Biochemical Pharmacology, Barts and the London School of Medicine and Dentistry, William Harvey Research Institute, Queen Mary University of London, London, EC1M 6BQ, UK.

Prof. Francesco Dell'Accio
f.dellaccio@qmul.ac.uk
Experimental medicine and Rheumatology, Barts and the London School of Medicine and Dentistry, William Harvey Research Institute, Queen Mary University of London, London, EC1M 6BQ, UK.

ABSTRACT

Cartilage defects repair poorly. Recent genetic studies suggest that WNT3a may contribute to cartilage regeneration, however the dense, avascular cartilage extracellular matrix limits its penetration and signaling to chondrocytes. Extracellular vesicles actively penetrate intact cartilage. This study investigates the effect of delivering WNT3a into large cartilage defects *in vivo* using exosomes as a delivery vehicle.

Exosomes were purified by ultracentrifugation from conditioned medium of either L-cells overexpressing WNT3a or control un-transduced L-cells, and characterized by electron microscopy, nanoparticle tracking analysis and marker profiling. WNT3a loaded on exosomes was quantified by western blotting and functionally characterized *in vitro* using the SUPER8TOPFlash reporter assay and other established readouts including proliferation and proteoglycan content. *In vivo* pathway activation was assessed using TCF/Lef:H2B-GFP reporter mice. Wnt3a loaded exosomes were injected into the knees of mice, in which large osteochondral defects were surgically generated. The degree of repair was histologically scored after 8 weeks.

WNT3a was successfully loaded on exosomes and resulted in activation of WNT signaling *in vitro*. *In vivo*, recombinant WNT3a failed to activate WNT signaling in cartilage, whereas a single administration of WNT3a loaded exosomes activated canonical WNT signaling for at least one week, and eight weeks later, improved the repair of osteochondral defects.

WNT3a assembled on exosomes, is efficiently delivered into cartilage and contributes to the healing of osteochondral defects.

Keywords: Exosomes, cartilage, WNT3a, drug delivery, joint repair.

Key messages

Chondral and osteochondral regeneration is currently achieved using cell preparations, usually autologous, which are expensive and laborious. We reported that a single administration of WNT-3A assembled on extracellular vesicles can enhance long term osteochondral regeneration. In addition we report that extracellular vesicles are an effective vehicle for the delivery of bioactive molecules through the abundant, negatively charged and avascular cartilage extracellular matrix.

Word count: 4229

INTRODUCTION

Cartilage defects are present in 61% of patients undergoing knee arthroscopy[1,2], can be disabling, and have the potential to progress into osteoarthritis[3]. Cell based approaches to cartilage repair are effective, but, due to the largely autologous nature of the transplanted cells, such procedures are costly and laborious. A number of novel biological agents are being developed which harness and support the endogenous capacity of joint to repair[4]. One major limitation in delivering such agents (often macromolecules) is the avascular nature of the cartilage tissue and the dense and strongly negatively charged extracellular matrix. Antibodies only penetrate the very superficial layers[5,6]. Our recent discovery that extracellular vesicles from neutrophils actively penetrate cartilage, suggests that extracellular vesicles may be ideal vehicles to deliver bioactive molecules to cartilage[7].

Extracellular vesicles are a heterogeneous group of double membrane bound vesicles, ranging in size from 30-400nm, and are synthesized either, through direct shedding from the plasma membrane (microvesicles), or by inward budding within multi-vesicular bodies (exosomes). They are naturally adapted to deliver their contents to cells, can target different tissues, are relatively stable in biological fluids and can travel over long distances. Understanding their potential and harnessing their targeting ability, would open an abundance of therapeutic opportunities in different disease areas and drug delivery[8].

As a proof of concept we chose to deliver WNT3a in a model of cartilage regeneration, because single nucleotide polymorphisms in the *WNT3a* gene are associated with a reduced regenerative capacity of ear lobe cartilage and because of the striking expression pattern of WNT3a at the cartilage regeneration front[9].

WNTs are a family of highly conserved signaling molecules that signal through a number of different pathways, including the β-catenin-dependent (canonical WNT) pathway, and are known to drive physiological processes including developmental morphogenesis, stem cell maintenance and wound healing[10,11].

WNT-β-catenin signaling is activated in response to joint and cartilage injury[12]. WNT3a is a strong activator of the WNT-β-catenin pathway[13,14]. In healthy cartilage, excessive activation of this pathway results in cartilage breakdown[13,15–17]; however following injury, when remodeling and cell expansion is necessary to repair tissue, appropriate and timely WNT3a upregulation was associated with improved repair[9]. WNTs are insoluble molecules that normally adhere to the cell surface through binding to heparansulphate proteoglycans. Some WNT molecules, however, can travel long distances assembled either with a carrier molecule called SWIM, or attached to the surface of exosomes[18].

Taking advantage of the capacity of WNT3a to be secreted naturally on the surface of exosomes we tested the hypothesis that exosomes are an effective vehicle to deliver biologically active molecules into cartilage and that exosome facilitated delivery of WNT3a would result in a long lasting protective effect and improve the repair of osteochondral defects in mice.

METHODS

Patients or the public were not involved in this research.

Isolation and characterisation of exosomes

Conditioned medium was generated using serum-free medium containing ITS supplement (Sigma I3146), as per the manufacturer's instructions from L-cells stably transfected with WNT3a and control L-cells (ATCC® CRL2647™/ CRL2648™). Briefly, cells were maintained in complete medium containing DMEM/F12 with 10% fetal bovine serum (FBS). L-cells containing WNT3a were maintained with 0.4mg/ml G418 for selection. For generation of conditioned medium, cells at 80-90% confluency were split in a 1:4 ratio into a new flask and cultured for 4 days in DMEM without FBS and containing 1x ITS supplement, (G418 was removed from the L-cells containing WNT3a). Medium was then removed and replaced with fresh medium for a further 3 days. Both batches of medium were then mixed and passed through a 40μm filter before exosome isolation.

Exosomes were isolated as previously described[18]. Briefly, conditioned medium was centrifuged sequentially at 300xg, 2000xg and 10,000xg to remove dead cells and debris with the supernatant taken forward to the next step. Exosomes were concentrated by ultra-centrifugation at 100,000xg for 3 hours. The exosome pellet was resuspended in PBS and the ultracentrifugation step repeated to wash the exosome preparation, before re-suspending the exosome pellet in 200ul of PBS for every 50ml of starting conditioned medium. Particle concentration was determined using the NanosightTM, NS300TM for nanoparticle tracking analysis. Other validation steps included electron microscopy, western blotting and reporter assay.

Western blotting

For analysis of exosomal preparations, equal volumes or particle concentrations were loaded on Tris-Glycine polyacrylamide gels, and transferred to nitrocellulose membrane for antibody probing.

Reporter assay

HEK293 cells were maintained in complete medium described above. Cells were plated in monolayer and transfected with SUPER8XTOPFlash TCF/LEF - firefly luciferase reporter plasmid (Addgene), using JetPRIME transfection reagent (Polyplus). Following 24 hours the medium was changed to serum-free medium containing ITS and stimulated for a further 24 hours before collection and analysis using Dual luciferase reporter assay system (Promega).

In vitro micromass culture and alcian blue staining for functional analysis

Human articular chondrocytes (<6 population doublings), were plated in dense cultures (2e7cells/ml) to allow matrix deposition. Experiments were conducted in serum-free medium containing ITS, over a period of 6 days. For IL-1β experiments, micromasses were cultured for 4 days in serum-free medium and stimulus added for the final 2 days. Micromasses were then fixed with methanol at -20 then stained with 0.5% Alcian blue 8GS (Carl Roth C.I. 74240), over-night. The following day the dye was extracted using 8M Guanidine HCL and the

proteoglycan content quantified using a spectrophotometer[19]. To account for any cell proliferation, total proteoglycans were normalised for DNA content.

QPCR for functional analysis

Human articular chondrocytes (<6 population doublings), were plated in monolayer and stimulated under serum-free conditions for 24 hours. RNA was extracted from cells using TRIzolTM reagent (Invitrogen 15596026), cDNA was then synthesized using oligo(dt) primers (Promega C1101) and SuperscriptTM III Reverse transcriptase (Invitrogen 18080093). QPCR analysis was performed for the desired genes. Primer sequences are as follows: Actin 5' TGACGGGGTCACCCACACTGTGCCCATCTA and 3' CTAGAAGCATTTGCGGTGGACGATGGAGG, Human Sox9 5' GAACGCACATCAAGACGGAG and 3' TCTCGTTGATTTCGCTGCTC, Human Aggrecan 5'GTTGTCATCAGCACCAGCATC and 3'ACCACACAGTCCTCTCCAGC, Human Col2a1 5'CTGCTCGTCGCCGCTGTCCTT and 3'AAGGGTCCCAGGTTCTCCATC, Human MMP13 5' ACGGACCCATACAGTTTGAATACAGC and 3' CCATTTGTGGTGTGGGAAGTATCATC. Human MMP3 5' CAACCGTGAGGAAAATCGATGCAG AND 3' CGGCAAGATACAGATTCACGCTCAA, Human MMP8 5'GTCATTGTTTCCCATCACTGTATCCATT AND 3' GGACACAATTCAACCCACGAAACA, Human PCNA 5' GGAGAACTTGGAAATGGAAAC AND 3' CTGCATTTAGAGTCAAGACCC.

***In vivo* models**

The *TCF/Lef:H2B-GFP* reporter line was donated by Anna-Katerina Hadjantonakis, Memorial Sloan-Kettering Cancer Center[20]. JAX stock #013752. For analysis of joint tissue penetration by exosomes, up to 7µl of exosome preparation or PBS vehicle was injected intra-articularly in the joints of adult transgenic mice expressing green fluorescence protein (GFP) under the control of the Tcf/Lef promoter (*TCF/Lef:H2B-GFP*)[20].

For analysis of joint tissue repair, ten week old, male C57BL/6 mice were anesthetized with isofluorane. A cylindrical defect (0.78+/- 0.042 mm wide and 1.79+/- 0.056 mm deep) was generated in the lateral femoral condyle using a 21gauge needle (Thomas, Eldridge et al. manuscript in preparation). Liquid rat collagen type 1 gel containing exosomes was injected using a pulled glass pipette tip with a diameter of approximately 10µm mounted at the end of a regular 2µl pipette tip until the defect was full. The gel solidifies at 37°C. The joint was closed with an interrupted suture. After recovery mice were left free to move and feed ad libitum in filter cages. The operator and the scorers were blind to the treatment. The animals were monitored for signs of suffering and local infection at least weekly. Mice were killed 8 weeks after injury and the joints taken for analysis.

Staining and immunofluorescence

Following dissection, mouse knees were fixed overnight with buffered 4% paraformaldehyde, then decalcified for 24 hours in formic acid buffer (33% formic acid, 13.5% trisodium citrate) at room temperature. Joints were than washed with water and embedded in OCT for cryosectioning (at 5µM). For proteoglycan analysis, sections were stained with 0.2% Safranin O in acetate buffer pH4. Safranin-O intensity was measured by densitometry analysis, performed using ImageJ software as previously described[21]. For immunofluorescence staining, sections were probed with anti-GFP antibody (Abcam ab290). Percentage GFP positive cells were calculated as the percentage of fluorescent cells over the total number of cells present in the area analysed.

The same approach was applied when quantifying the percentage of Ki67 positive cells, which were fixed with 4% paraformaldehyde and stained with Ki67 antibody (Abcam 15580) and dapi.

Ethics

Animal experiments were conducted under Home Office license 70/7986. Human samples were approved and obtained under the East London and the city research ethics commitee3 (Rec N.07/Q0605/29). Adult human articular cartilage was obtained from patients undergoing joint replacement for knee OA after obtaining informed consent.

Statistical analysis

Parametric data were compared with the t-test, non-parametric data with the Mann–Whitney test. Paired analysis was used for *in vivo* comparisons, where controls were contralateral knees. For multiple comparisons, an ANOVA or Kruskal-Wallis, including the Tukey's post-test, was used. P-Values <0.05 were considered significant: $*p<0.05$;$**p<0.01$;$***p<0.001$.

RESULTS

WNT3a inhibits specific functions of IL-1β in chondrocytes

Excessive activation of WNT-β-catenin signaling results in loss of cartilage extracellular matrix; nevertheless, WNT3a expression at the injury site facilitates repair[9]. We hypothesised that WNT3a may result in different outcomes in chondrocytes, depending on whether they are in resting conditions or during conditions of challenge. To test this hypothesis we assessed the effect of recombinant WNT3a (R-WNT3a), on cartilage catabolism in resting chondrocytes and in the presence of an inflammatory stimulus, Interleukin-1β (IL-1β). As expected, R-WNT3a treatment of human articular chondrocytes (HAC), in micromass culture, resulted in a reduction in proteoglycan content (Fig.1A). IL-1β treatment decreased proteoglycan content to an even greater extent, however co-treatment with WNT3a lead to a partial rescue of IL-1β - induced proteoglycan loss (Fig.1A). In keeping with this, R-WNT3a like IL-1β caused a loss of chondrocyte markers *COL2a1* and *AGGRECAN*, as well master transcription regulator of cartilage, *SOX9*, but was able to inhibit matrix-metalloprotease-13 (*MMP-13*) upregulation caused by IL-1β. Under these experimental conditions however, WNT3a did not show the same effect on other MMPs upregulated by IL-1β such as MMP-3 and MMP-8 (Fig.1B). These results encouraged us to explore the use of WNT3a to support cartilage repair.

WNT3a is transferred and carried on exosomes

WNTs are palmitoylated, rendering them insoluble[22]. In order to overcome this, and to allow long-distance signaling, endogenous WNTs are secreted from cells on the surface of exosomes or associated with other carrier molecules such as SWIM [18]. Since we previously demonstrated that extracellular vesicles actively enter the cartilage matrix[7], we tested whether we could use extracellular vesicles to deliver WNT3a to chondrocytes. This was facilitated by the fact that overexpressed WNT3a is spontaneously assembled and secreted on the external surface of exosomes as previously demonstrated by electron microscopy and immunogold labeling [18,23]. WNT3a-containing exosomes (Ex-WNT3a) or control exosomes (Ex-C) were purified by ultracentrifugation from conditioned medium generated from well-established cell lines, L-cells stably expressing WNT3a (L-WNT3a)[18], or from control L-cells (Fig.2). Exosomes had the expected shape and size distribution and no major differences were observed between the two populations, as assessed by electron microscopy and nanoparticle tracking analysis (Fig.2A+B). Although the number of exosome batches produced was too low to allow proper statistical analysis, we did not observe any differences in size or the ratio of exosomes produced between treatments or across different batches of exosomes, generated at different times (Fig.2B iii). The exosome preparation contained the exosomal marker TSG101 (Fig.2C)[18]. WNT3a could be detected on exosomes generated from L-WNT3a cells but not on those generated from control L-cells (Fig.2C). By comparison with a standard curve generated with known amounts of R-WNT3a, we could estimate that the concentration of WNT3a in the exosomal preparation was 0.0043pg/particle (Fig.2D and Supplementary Fig.1). An equal number of Ex-c and Ex-WN3a particles were compared in all functional assays.

Exosomes can deliver functionally active WNT3a into cartilage *in vitro*.
Ex-WNT3a for *in vitro* experiments were administered in order to dose either an estimated 100ng/ml or 50ng/ml of exosome associated WNT3a for comparison against the same concentration of recombinant WNT3a. To assess whether WNT3a was expressed on exosomes in an active form, we tested whether Ex-WNT3a could activate the WNT-β-catenin dependent SUPER8TOPFlash reporter assay in HEK293 cells. These experiments showed, not only that Ex-WNT3a efficiently activated the reporter assay, but that Ex-WNT3a activity was maintained also in serum-free conditions. Whereas R-WNT3a was inactive in the absence of serum, presumably due to its poor solubility[22] (Fig.3A). This suggested that exosomes are efficient carriers for WNTs and deliver them in a format that enables signaling. Next we tested whether the exosomal delivery of WNT3a modulates its functional activity. We chose the following biological outcomes to test: chondrocyte proliferation and reduction of proteoglycan content[13]. *In vitro,* Ex-WNT3a upregulated markers of proliferation, including *PCNA* mRNA and Ki67 protein (Fig.3B+C). Importantly, Ex-WNT3a induced greater proliferation than an equivalent amount of the R-WNT3a. This further confirms results seen in figure 3A, that WNT molecules do not signal efficiently in the absence of serum, but transport on exosomes is able to overcome this problem. To validate that Ex-WNT3a had the same protective effects as R-WNT3a (Fig.1A), we treated HAC micromasses with IL-1β and/or equal concentration of Ex-WNT3a. Interestingly Ex-WNT3a alone, did not induce loss of proteoglycan of the HAC micromass (Fig.3D). This is in contrast with that seen for R-WNT3a (Fig.1A). When administered in combination with IL-1β however, which caused a decrease in proteoglycan content, similarly to the recombinant protein, Ex-WNT3a resulted in a slight but significant rescue (Fig.3D).

Exosomes can penetrate cartilage tissue and deliver biologically active WNT3a *in vivo*.
To assess whether exosomes could deliver active WNT3a into the cartilage matrix and signal to chondrocytes *in vivo* we used a TCF/Lef:H2B-GFP transgenic mouse line. These mice express green fluorescence protein (GFP) under the control of the Tcf/Lef promoter (TCF/Lef:H2B-GFP)[20]. Since Tcf/Lef is a sensitive target of WNT-β-catenin signaling, GFP becomes expressed in cells in which signaling is activated. As WNT3a is a potent activator of the WNT-β-catenin pathway, a strong induction of GFP was expected upon WNT3a delivery. Stimulus was administered intra-articularly, to ensure that exosomes reached the cartilage within the joint. The joint cavity has a relatively low volume and therefore limits the amount of liquid that can be injected (up to 7μl). We administered the maximum volume possible to ensure sufficient concentrations of WNT3a, which dictated the number of exosomes particles administered. This resulted in the administration of an estimated 18ng of WNT3a (4.2e6 particles for both Ex-WNT3a and Ex-C) at the 2 day end point, and 44ng of WNT3a (10.1e6 particles of Ex-WNT3a compared to PBS vehicle) at the 4 and 7 day endpoints. 44ng of recombinant WNT3a was administered. *In vivo*, the intra-articular injection of Ex-WNT3a in TCF/Lef:H2B-GFP reporter mice (Fig.4A) resulted in the activation of WNT-β-catenin signaling within the full thickness of the articular cartilage and menisci as assessed by immunofluorescence for GFP (Fig.4B). Importantly the same concentration of R-WNT3a, failed to activate the

GFP reporter (Fig.4C). In keeping with the known capacity of WNT3a to reduce glycosaminoglycan in cartilage tissue[13], Safranin-O staining was reduced in the cartilage of mice treated with Ex-WNT3a, 7 days post injection (Fig.4D).

Exosomes loaded with WNT3a improved osteochondral repair in mice.

WNT3a is genetically associated with the capacity to repair the ear lobe in mice[9]. To investigate if Ex-WNT3a enhanced the repair of osteochondral defects in the knee, we generated critical-size osteochondral defects on the lateral femoral condyle of adult mice and filled it with rat collagen type1 gel containing either Ex-WNT3a or Ex-C (Fig.5A). As with previous *in vivo* investigations (Fig.4) we administered the maximum number of particles possible into the volume of the defect, resulting in an estimated 5ng of WNT3a delivered (1.2e6 particles for both Ex-C and Ex-WNT3a). Eight weeks later, joints treated with Ex-WNT3a had an improved repair score (measured by the Pineda score[24]), when compared to joints treated with Ex-C (Fig.5B+C). Histological images show an overview of the joint (Fig.5B), a higher magnification of the cartilage surface in the region of the defect (Fig.5B i), and a higher magnification of the synovial lining (Fig.5B ii), which at this late endpoint, showed no hyperplasia/ thickening of the synovial lining. In a second experiment, we repeated the defect and treatment regime but this time terminated at only 3 days post injury to assess the situation in the joints during the early phases of repair. No visible histological differences were observed at this stage, between joints treated with either Ex-C or Ex-WNT3a (representative images shown in supplementary figure 2). However cartilage surface/joint damage, consistent with the early phases following injury, were observed in all joints and are represented in Fig.5D. Histological images show an overview of an injured knee joint, with insets showing damaged cartilage/ subchondral bone tissues in the outer regions of the defect (Fig.5 i), cartilage surface fibrillation in regions of the joint away from the defect (Fig.5 ii), and thickening of the synovial lining (Fig.5 iii), consistent with the expected inflammation present at this early stage following injury.

DISCUSSION

We have shown that the use of exosomes as a vehicle enables the delivery of WNT3a into the avascular cartilage in a biologically active form and promotes the healing of critical size osteochondral defects in mice.

Chondrocytes are encased in a dense, negatively charged, avascular extracellular matrix, which is poorly permeable to macromolecules. For instance, antibodies do not penetrate the cartilage extracellular matrix[25] and even antigen binding fragments only enter the very superficial layers[26]. In addition, WNT molecules are relatively insoluble[27] and bind to heparansulphate proteoglycans which can further reduce their passive diffusion into cartilage. In view of this, it is not surprising that the injection of recombinant WNT3a did not elicit a signaling response.

In contrast, we have provided evidence that exosomes achieve efficient and prolonged delivery of this particularly challenging molecule, into the full depth of the cartilage. This represents a technological breakthrough for several molecular targets that have been validated using transgenic approaches in repair as well as in osteoarthritis[28–36], but where the efficient delivery of a recombinant protein is an obstacle towards clinical application.

Extracellular vesicles have the advantage over synthetic carriers such as liposomes or capsules in that they have active mechanisms of motility and homing. For instance, extracellular vesicles, but not capsules of the same size could penetrate the avascular cartilage extracellular matrix and reach chondrocytes[7]. In recent years the potential of exosomes as delivery vehicles has been well recognized and interest from the pharmaceutical industry has soared resulting in technological advancements in the field. These include breakthroughs in loading and delivery of cargo[37] as well as improvements and up scaling for production and purification. In this study we chose ultracentrifugation for exosome preparation, this is in adherence with previous reports studying the secretion of WNTs on exosomes[18,23]. Although widely used, when considering large scale production and preparation, limitations such as the co-isolation of non EV materiel and the tedious nature of the technique for low recovery of product, makes the method unsuitable. Novel and improved technologies, will therefore be essential when considering exosomes for therapy. In addition to production, challenges in bringing these novel EV based therapeutics to the clinic will also need to be overcome. It is likely that given their cellular origin and complex composition, they will require an approach similar to that of cell based therapies[38]. Never the less, utilizing and expanding on this opportunity to overcome challenges in delivering therapy to cartilage, in the future could lead to safe and efficient production of exosomes from validated cell lines for delivery of even large complicated molecules, thus removing one of the biggest challenges in treating cartilage injury.

We previously showed that extracellular vesicles actively penetrate the cartilage extracellular matrix[7]. It is not clear whether this active penetration is due to adhesion properties and motility or whether the extracellular vesicles follow

chemotactic cues. Here we showed the successful delivery of a WNT3a signal by exosomes, to chondrocytes within their extracellular matrix, however, we did not demonstrate that the exosomes physically enter the matrix and reach the chondrocyte cell membrane. It is therefore also possible that WNTs are released from the exosomes before entering cartilage or that they trigger relay mechanisms. The delivery of WNT3a on exosomes led to a surprisingly long-lasting signaling response, suggesting that the exosomes not only conferred WNT3a signal into the cartilage, but also may prolong the local half-life.

It is important to highlight how a single delivery of exosomal WNT3a was sufficient to improve repair, which was evident 8 weeks later. We did not observe any differences between Ex-WNT3a and Ex-C treated knees at 3 days post injury, and therefore, cannot confirm a precise mechanism of action for Ex-WNT3a in joint repair. It is possible that the huge endogenous response occurring in the joint following injury, could mask differences between treatments. Considering the biology of WNT3a, and our WNT pathway activation data in healthy mouse knees (Fig.4), we can hypothesise that the long-lasting effect was due to the retention of WNT3a in an active form for prolonged or increased signaling. It is also possible that a relatively short signaling event by WNT3a may have triggered homeostatic effects that are self-maintained or lead to long-term outcomes. This is suggested by the fact that a single, short episode of activation of β-catenin led to the formation of thicker cartilage in mice[39].

Whereas there is abundant literature covering the genetics of osteoarthritis, the genetics of repair are understudied. A recent publication identified a single nucleotide polymorphism in the Wnt3a locus which was associated with the capacity of mouse sub-strains to repair punch-holes in the ear pinna[9]. In keeping with a direct function in repair mechanism, WNT3a protein was more strongly expressed at the healing edge of the ear cartilage in mouse strains that healed better. This, and the capacity of WNT3a to profoundly modulate the chondrocyte phenotype[13] motivated our choice for this target.

Our data show that WNT3a was able to drive an improved repair following joint injury (figure 5). In spite of this, and the genetic evidence supporting a positive role of WNT3a in cartilage repair and its well-known capacity to support cartilage stem cells[14], WNT3a is also known to mediate catabolic functions such as loss of extracellular matrix components (figure 1 and reference[13]). This apparent paradox is explained by the fact that joint surface repair requires a sequence of events in a precise, tightly regulated temporal order. The early phases immediately after injury are characterized by expansion of stem cell populations[3,40] and extracellular matrix remodelling[3,12,41]. The late phases, instead, are characterized by tissue patterning followed by extracellular matrix synthesis and maturation[42]. The choice of therapeutic agents to enhance repair, therefore, will need to be targeted to the specific repair phase. In this context, we chose to deliver WNT3a in the early phase of repair when matrix remodeling and cell proliferation are required to replace damaged cells and tissues, rather than in the later phases when WNT3a may result in detrimental effects such as loss of proteoglycans. In healthy cartilage WNT signaling needs to be maintained to a minimum, whereas cartilage injury triggers a transient wave

of WNT activation[12,43] which is required to support local progenitor cells [39]. Therefore, while administering WNT3a to recently injured cartilage reinforced a naturally occurring repair mechanism which ultimately led to increased proteoglycan content, its administration in healthy cartilage triggered a early, likely transient, matrix remodeling, which would be useful during the early phases of repair, but is undesirable in homeostatic conditions.

In keeping with this observation, in our experiments, recombinant WNT3a had a dramatically different effect in healthy cartilage (in which it drove the loss of extracellular matrix), compared to inflammatory conditions (in which it reduced the capacity of IL-1β to cause loss of proteoglycans) (figure 1). Interestingly, unlike recombinant WNT3A, WNT3A associated to exosomes did not result in proteoglycan loss in chondrocyte micromasses (figure 3D). While we do not have experimental data do explain this discrepancy, it is possible that the context of WNT3a presentation when assembled on exosomes may modify its affinity to its receptors and bias its signaling properties. Alternatively, the bioavailability of WNT3a assembled on exosomes may be different or be associated with different temporal dynamics compared to the naked recombinant protein.

Although, in our murine injury model, we could measure a statistically significant improvement of the repair outcome, the quality of the healed cartilage was not optimal. This could be due to different factors, including the size of the defect, which might be too large to achieve full repair, the dose of WNT3a, the time and frequency of administration, and the choice of the bioactive molecule being delivered. In this context, although our choice of WNT3a was justified by genetic evidence, other WNTs such as WNT16, which supports production of the joint lubricant, Lubricin[21], have shown perhaps a better pharmacological profile. Nevertheless, this study represents a unique proof of concept that supporting the early phases of repair has long term beneficial outcomes. This study also represents a proof of concept for this technology. The choice of the ligand, the generation of appropriate cell lines for exosome generation, and safe, optimal, consistent delivery, will be paramount for the clinical application.

In this study we have demonstrated that a single administration of WNT3a, a molecule upregulated by acute cartilage injury, enhances the long-term outcome of cartilage repair. This highlights the importance of the early phases of injury response in priming the repair cascade. In addition, we have demonstrated that exosomes are able to deliver functionally active molecules into joint tissues, resulting in long lasting and protective effects. This presents a unique opportunity to harness the natural targeting power of exosomes for the benefit of therapy delivery across medicine.

ACKNOWLEDGEMENTS AND FUNDING

We kindly thank our funders: UCB pharma, MRC (grants MR/P026362/1, MR/R000956/1, MR/N010973/1), Versus Arthritis (grants 21621, 21515), William Harvey Research Foundation and the European Region Action Scheme for the Mobility of University Students (ERASMUS) program.

AUTHOR CONTRIBUTIONS

FDA and BLT incepted the study. BLT, FDA, SEE, RJ, AMo, AMa, GN, SEE, A-ST, SC and CP contributed to experimental design. BLT, FDA, SEE, BN, MA, A-ST, SC, AB, JGN performed the experimental work. BLT, FDA, RJ, AMo, AMa, A-ST, SC, SEE and CG-M interpreted results. BLT, FDA, AMa, contributed to writing and completion of the manuscript. MP provided infrastructural support.

COMPETING INTERESTS

The Authors declare no conflict of interest

REFERENCES

1 Curl WW, Krome J, Gordon ES, *et al.* Cartilage injuries: A review of 31,516 knee arthroscopies. *Arthrosc J Arthrosc Relat Surg* 1997;**13**:456–60. doi:10.1016/S0749-8063(97)90124-9

2 Hjelle K, Solheim E, Strand T, *et al.* Articular cartilage defects in 1,000 knee arthroscopies. *Arthrosc J Arthrosc Relat Surg* 2002;**18**:730–4. doi:10.1053/JARS.2002.32839

3 Dell'accio F, Vincent TL. Joint surface defects: clinical course and cellular response in spontaneous and experimental lesions. *Eur Cell Mater* 2010;**20**:210–7.http://www.ncbi.nlm.nih.gov/pubmed/20878619

4 Sherwood J. Osteoarthritis year in review 2018: biology. *Osteoarthr Cartil* 2019;**27**:365–70. doi:10.1016/j.joca.2018.10.005

5 DiDomenico CD, Xiang Wang Z, Bonassar LJ. Cyclic Mechanical Loading Enhances Transport of Antibodies Into Articular Cartilage. *J Biomech Eng* 2016;**139**:11012. doi:10.1115/1.4035265

6 DiDomenico CD, Goodearl A, Yarilina A, *et al.* The Effect of Antibody Size and Mechanical Loading on Solute Diffusion Through the Articular Surface of Cartilage. *J Biomech Eng* 2017;**139**:91005. doi:10.1115/1.4037202

7 Headland SE, Jones HR, Norling L V., *et al.* Neutrophil-derived microvesicles enter cartilage and protect the joint in inflammatory arthritis. *Sci Transl Med* 2015;**7**:315ra190-315ra190. doi:10.1126/scitranslmed.aac5608

8 EL Andaloussi S, Mäger I, Breakefield XO, *et al.* Extracellular vesicles: biology and emerging therapeutic opportunities. *Nat Rev Drug Discov* 2013;**12**:347–57. doi:10.1038/nrd3978

9 Cheverud JM, Lawson HA, Bouckaert K, *et al.* Fine-mapping quantitative trait loci affecting murine external ear tissue regeneration in the LG/J by SM/J advanced intercross line. *Heredity (Edinb)* 2014;**112**:508–18. doi:10.1038/hdy.2013.133

10 Burgy O, Königshoff M. The WNT signaling pathways in wound healing and fibrosis. *Matrix Biol* 2018;**68–69**:67–80. doi:10.1016/J.MATBIO.2018.03.017

11 Nusse R, Clevers H. Wnt/β-Catenin Signaling, Disease, and Emerging Therapeutic Modalities. *Cell* 2017;**169**:985–99. doi:10.1016/J.CELL.2017.05.016

12 Dell'accio F, De Bari C, Eltawil NM, *et al.* Identification of the molecular response of articular cartilage to injury, by microarray screening: Wnt-16 expression and signaling after injury and in osteoarthritis. *Arthritis Rheum*

2008;**58**:1410–21. doi:10.1002/art.23444
13 Nalesso G, Sherwood J, Bertrand J, *et al.* WNT-3A modulates articular chondrocyte phenotype by activating both canonical and noncanonical pathways. *J Cell Biol* 2011;**193**:551–64. doi:10.1083/jcb.201011051
14 Yasuhara R, Ohta Y, Yuasa T, *et al.* Roles of β-catenin signaling in phenotypic expression and proliferation of articular cartilage superficial zone cells. *Lab Invest* 2011;**91**:1739–52. doi:10.1038/labinvest.2011.144
15 Luyten FP, Tylzanowski P, Lories RJ. Wnt signaling and osteoarthritis. *Bone* 2009;**44**:522–7. doi:10.1016/j.bone.2008.12.006
16 Loughlin J, Dowling B, Chapman K, *et al.* Functional variants within the secreted frizzled-related protein 3 gene are associated with hip osteoarthritis in females. *Proc Natl Acad Sci U S A* 2004;**101**:9757–62. doi:10.1073/pnas.0403456101
17 Zhu M, Tang D, Wu Q, *et al.* Activation of β-Catenin Signaling in Articular Chondrocytes Leads to Osteoarthritis-Like Phenotype in Adult β-Catenin Conditional Activation Mice. *J Bone Miner Res* 2009;**24**:12–21. doi:10.1359/jbmr.080901
18 Gross JC, Chaudhary V, Bartscherer K, *et al.* Active Wnt proteins are secreted on exosomes. *Nat Cell Biol* 2012;**14**:1036–45. doi:10.1038/ncb2574
19 De Bari C, Dell'Accio F, Luyten FP. Human periosteum-derived cells maintain phenotypic stability and chondrogenic potential throughout expansion regardless of donor age. *Arthritis Rheum* 2001;**44**:85–95. doi:10.1002/1529-0131(200101)44:1<85::AID-ANR12>3.0.CO;2-6
20 Ferrer-Vaquer A, Piliszek A, Tian G, *et al.* A sensitive and bright single-cell resolution live imaging reporter of Wnt/ß-catenin signaling in the mouse. *BMC Dev Biol* 2010;**10**:121. doi:10.1186/1471-213X-10-121
21 Nalesso G, Thomas BL, Sherwood JC, *et al.* WNT16 antagonises excessive canonical WNT activation and protects cartilage in osteoarthritis. *Ann Rheum Dis* 2016;:annrheumdis-2015-208577. doi:10.1136/annrheumdis-2015-208577
22 Willert K, Brown JD, Danenberg E, *et al.* Wnt proteins are lipid-modified and can act as stem cell growth factors. *Nature* 2003;**423**:448–52. doi:10.1038/nature01611
23 Koch R, Demant M, Aung T, *et al.* Populational equilibrium through exosome-mediated Wnt signaling in tumor progression of diffuse large B-cell lymphoma. *Blood* 2014;**123**:2189–98. doi:10.1182/blood-2013-08-523886
24 Pineda S, Pollack A, Stevenson S, *et al.* A semiquantitative scale for histologic grading of articular cartilage repair. *Acta Anat (Basel)* 1992;**143**:335–40.http://www.ncbi.nlm.nih.gov/pubmed/1502876 (accessed 16 May 2019).
25 Maroudas A. Transport of solutes through cartilage: permeability to large molecules. *J Anat* 1976;**122**:335–47.http://www.ncbi.nlm.nih.gov/pubmed/1002608 (accessed 16 May 2019).
26 Byun S, Sinskey YL, Lu YCS, *et al.* Transport of anti-IL-6 antigen binding fragments into cartilage and the effects of injury. *Arch Biochem Biophys* 2013;**532**:15–22. doi:10.1016/j.abb.2012.12.020

27 Fuerer C, Habib SJ, Nusse R. A study on the interactions between heparan sulfate proteoglycans and Wnt proteins. *Dev Dyn* 2010;**239**:184–90. doi:10.1002/dvdy.22067
28 Araldi E, Khatri R, Giaccia AJ, *et al.* Lack of HIF-2α in limb bud mesenchyme causes a modest and transient delay of endochondral bone development. *Nat Med* 2011;**17**:25–6. doi:10.1038/nm0111-25
29 Glasson SS, Askew R, Sheppard B, *et al.* Deletion of active ADAMTS5 prevents cartilage degradation in a murine model of osteoarthritis. *Nature* 2005;**434**:644–8. doi:10.1038/nature03369
30 Johnson K, Zhu S, Tremblay MS, *et al.* A stem cell-based approach to cartilage repair. *Science* 2012;**336**:717–21. doi:10.1126/science.1215157
31 Kim J-H, Jeon J, Shin M, *et al.* Regulation of the Catabolic Cascade in Osteoarthritis by the Zinc-ZIP8-MTF1 Axis. *Cell* 2014;**156**:730–43. doi:10.1016/j.cell.2014.01.007
32 Monteagudo S, Cornelis FMF, Aznar-Lopez C, *et al.* DOT1L safeguards cartilage homeostasis and protects against osteoarthritis. *Nat Commun* 2017;**8**:15889. doi:10.1038/ncomms15889
33 Sampson ER, Hilton MJ, Tian Y, *et al.* Teriparatide as a Chondroregenerative Therapy for Injury-Induced Osteoarthritis. *Sci Transl Med* 2011;**3**:101ra93-101ra93. doi:10.1126/scitranslmed.3002214
34 Xie L, Tintani F, Wang X, *et al.* Systemic neutralization of TGF-β attenuates osteoarthritis. *Ann N Y Acad Sci* 2016;**1376**:53–64. doi:10.1111/nyas.13000
35 Xu L, Servais J, Polur I, *et al.* Attenuation of osteoarthritis progression by reduction of discoidin domain receptor 2 in mice. *Arthritis Rheum* 2010;**62**:2736–44. doi:10.1002/art.27582
36 Zhen G, Wen C, Jia X, *et al.* Inhibition of TGF–β signaling in subchondral bone mesenchymal stem cells attenuates osteoarthritis. *Nat Med* 2013;**19**:704. doi:10.1038/NM.3143
37 Heath N, Osteikoetxea X, de Oliveria TM, *et al.* Endosomal escape enhancing compounds facilitate functional delivery of extracellular vesicle cargo. *Nanomedicine* 2019;**14**:2799–814. doi:10.2217/nnm-2019-0061
38 Lener T, Gimona M, Aigner L, *et al.* Applying extracellular vesicles based therapeutics in clinical trials - An ISEV position paper. *J Extracell Vesicles* 2015;**4**:4. doi:10.3402/jev.v4.30087
39 Yuasa T, Kondo N, Yasuhara R, *et al.* Transient activation of Wnt/{beta}-catenin signaling induces abnormal growth plate closure and articular cartilage thickening in postnatal mice. *Am J Pathol* 2009;**175**:1993–2003. doi:10.2353/ajpath.2009.081173
40 Roelofs AJ, Zupan J, Riemen AHK, *et al.* Joint morphogenetic cells in the adult mammalian synovium. *Nat Commun* 2017;**8**:15040. doi:10.1038/ncomms15040
41 Sherwood JC, Bertrand J, Eldridge SE, *et al.* Cellular and molecular mechanisms of cartilage damage and repair. *Drug Discov Today* 2014;**19**:1172–7. doi:10.1016/j.drudis.2014.05.014
42 Eltawil NM, De Bari C, Achan P, *et al.* A novel in vivo murine model of cartilage regeneration. Age and strain-dependent outcome after joint surface injury. *Osteoarthritis Cartilage* 2009;**17**:695–704. doi:10.1016/j.joca.2008.11.003

43 Dell'Accio F, De Bari C, El Tawil NMF, *et al.* Activation of WNT and BMP signaling in adult human articular cartilage following mechanical injury. *Arthritis Res Ther* 2006;**8**:R139. doi:10.1186/ar2029

FIGURE LEGENDS

Figure 1: A) HAC micromasses were treated with combinations of recombinant WNT3a (50ng/ml R-WNT3a) and IL1-β (10ng/ml) over 6 days, then stained with alcian blue (Ab) dye to assess proteoglycan content, which was normalised to DNA content to account for proliferation (n=4). B) HAC were treated with IL1-β (10ng/ml) and R-WNT3a (100ng/ml) and mRNA readouts of cartilage anabolism and IL1-β pathway activation assessed by QPCR after 24 hours (n=4).

Figure 2: A) Electron microscopy of Ex-WNT3a and Ex-C. Includes an overview and zoomed in images. Scale bars on all images represent 0.2μm. B i and ii) Nanoparticle tracking analysis of representative Ex-WNT3a and Ex-C preparations using NanosightTM(NS300). B iii) Comparison of number of particles and modal size of the particles (nm) for both Ex-C and Ex-ENT3a across different batches. C) Western blot for WNT3a and Tsg101 (exosomal marker) of 20ul of supernatant (SNo) and exosome pellet/fraction (Ex fract) of L-WNT3a and control L-cells, following 100,000xg ultracentrifugation (n=2). D) Western blot for WNT3a using a standard curve of R-WNT3a ([Rec]) and varying amounts of Ex-WNT3a ([Ex]) to determine concentration of WNT3a in exosome preparation (n=3). Detailed explanation in supplementary figure 1.

Figure 3: A) SUPER8TOPFlash reporter assay in HEK293 cells comparing R-WNT3a and Ex-WNT3a, both serum and serum-free conditions (estimated 100ng/ml WNT3a, n=4). B) HAC were treated with Ex-WNT3a, Ex-C, R-WNT3a or PBS, for 24 hours in serum-free conditions (estimated 100ng/ml WNT3a). QPCR for *PCNA* mRNA was conducted (n=4). C) HAC from two separate donors, were treated with Ex-WNT3a (50ng/ml) and equal concentration of R-WNT3a for 24 hours in serum-free conditions. Cells were stained for Ki67 protein to assess cell proliferation (n=8 per donor). Representative pictures for Ki67 analysis shown below. D) HAC micromasses were treated with combinations of Ex-WNT3a (50ng WNT3a protein) and IL1-β (10ng/ml) over 6 days in serum-free conditions, then stained with alcian blue dye to assess proteoglycan content (n=4).

Figure 4: A) Immunofluorescence for GFP in TCF/Lef:H2B-GFP reporter mice injected intra-articularly with Ex-WNT3a or Ex-C (representative images from the 2 day end point). B) Quantification of immunofluorescence for GFP in TCF/Lef:H2B-GFP mice injected with Ex-WNT3a or control and killed after 2, 4 and 7 days (n=4 per time point). For the 2-day end point, Ex-WNT3a containing 18ng of WNT3a was compared to an equal particle number of Ex-C (4.2e6 particles). In the 4 and 7-day end point, Ex-WNT3a containing 44ng of WNT3a (10.1e6 particles) was compared to contralateral control knees injected with PBS vehicle. C) Additional reporter mice were injected with 44ng of WNT3a recombinant and compared to their contralateral controls. D) Safranin-O staining of mice injected with Ex-WNT3a (containing 44ng of WNT3a) or PBS and killed 7 days later (n=4).

Figure 5: An osteochondral defect was generated in the lateral femoral condyle and filled with 2μl of rat collagen type1 gel, containing treatment. A) Scheme of

joint injury model, including images of time 0 and 8 weeks post injury (WPI) without treatment. B) Defects were treated with either Ex-WNT3a (estimated 5ng WNT3a protein) or Ex-C (equivalent number of particles, 1.2e6 particles per knee) at time 0 and the experiment was terminated at 8 WPI (n=7 for Ex-C and n=5 for Ex-WNT3a). Knees were sectioned and stained with Safranin-O. Defect margins are depicted by black brackets in over view images. Higher magnification images are shown in i (defect area at cartilage surface) and ii (synovium), with black arrows indicating synovial lining. C) Repair was assessed using the Pineda score at 8 WPI. D) Additional mice were treated exactly as in the 8 week experiment and instead terminated at 3 days post injury to assess the early phases of repair. Images show an overview of the injured joint and insets at a higher magnification: i) showing the cartilage surface in the area of the defect, ii) showing fibrillation on the cartilage surface away from the defect, and iii) showing proliferation in the synovial lining.

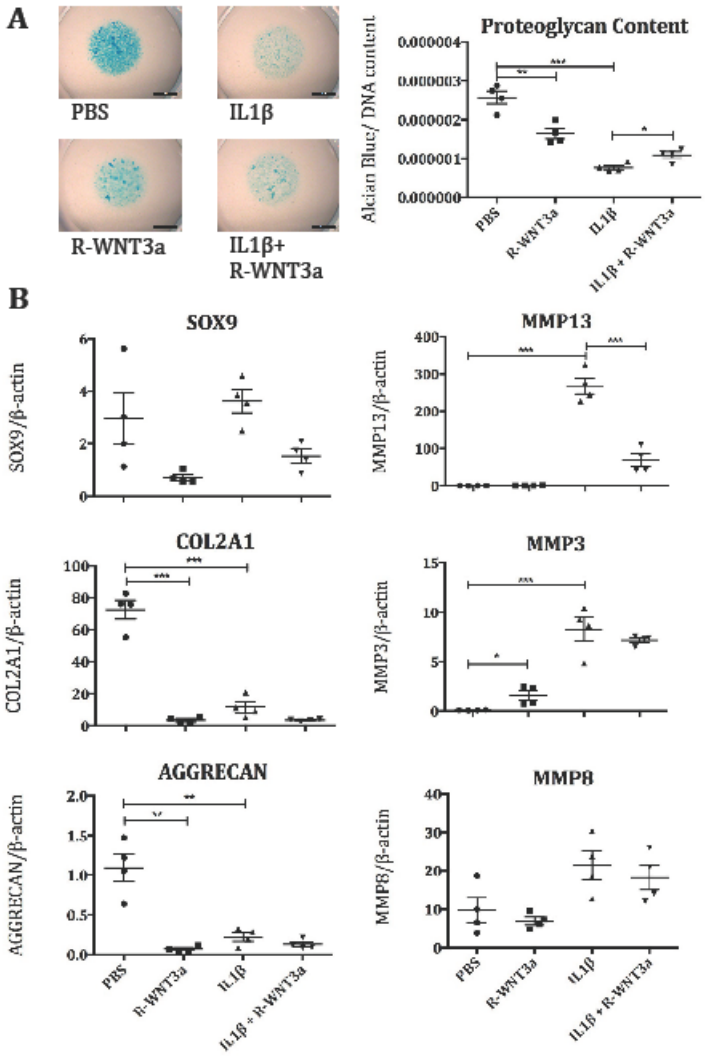
A
PBS
IL1β
R-WNT3a
IL1β+
R-WNT3a
Proteoglycan Content
Alcian Bluc/ DNA content
PBS
R-WNT3a
IL1β
IL1β + R-WNT3a
B
SOX9
SOX9/β-actin
MMP13
MMP13/β-actin
COL2A1
COL2A1/β-actin
MMP3
MMP3/β-actin
AGGRECAN
AGGRECAN/β-actin
MMP8
MMP8/β-actin

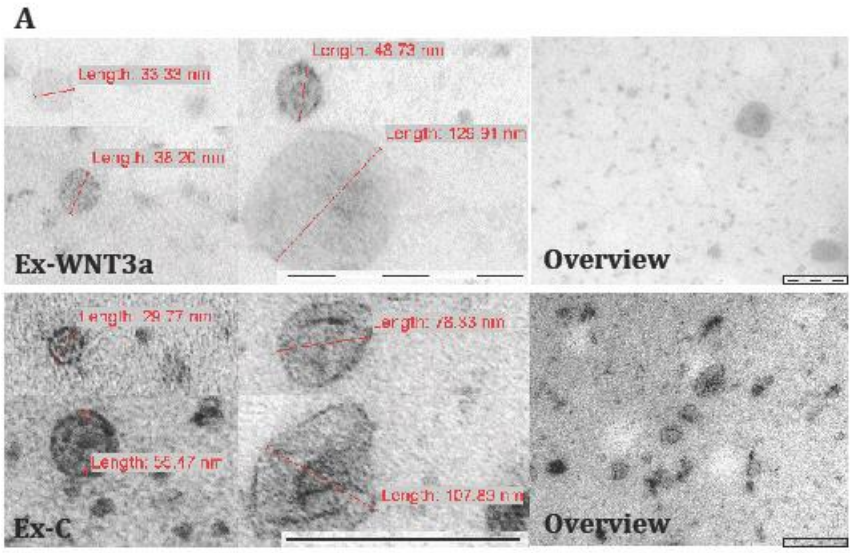
A
Length: 33.32 nm
Length: 48.73 nm
Length: 38.20 nm
Length: 125.91 nm
Ex-WNT3a
Overview
Length: 29.77 nm
Length: 78.33 nm
Length: 55.17 nm
Length: 107.89 nm
Ex-C
Overview

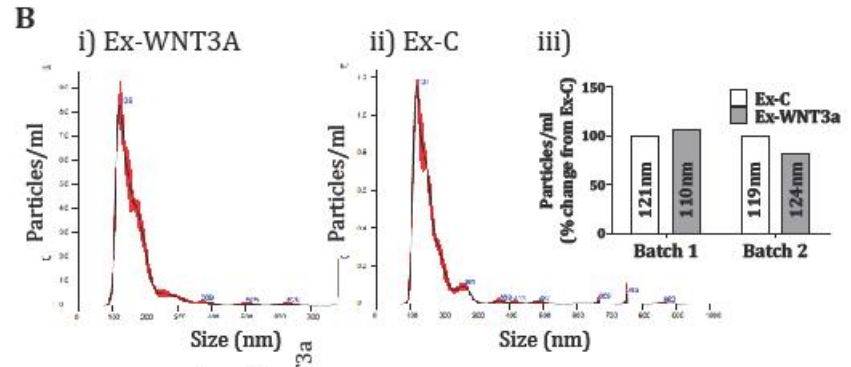
B
i) Ex-WNT3A
ii) Ex-C
iii)
Particles/ml
Size (nm)
Particles/ml
Size (nm)
Particles/ml (% change from Ex-C)
Ex-C
Ex-WNT3a
121nm
110nm
119nm
124nm
Batch 1
Batch 2

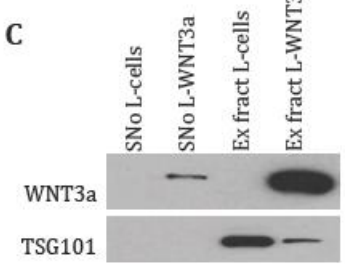
C
SNo L-cells
SNo L-WNT3a
Ex fract L-cells
Ex fract L-WNT3a
WNT3a
TSG101

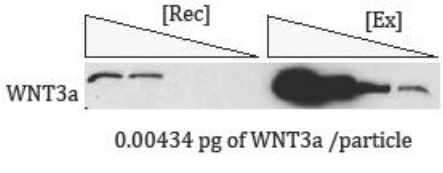
D
[Rec]
[Ex]
WNT3a
0.00434 pg of WNT3a /particle

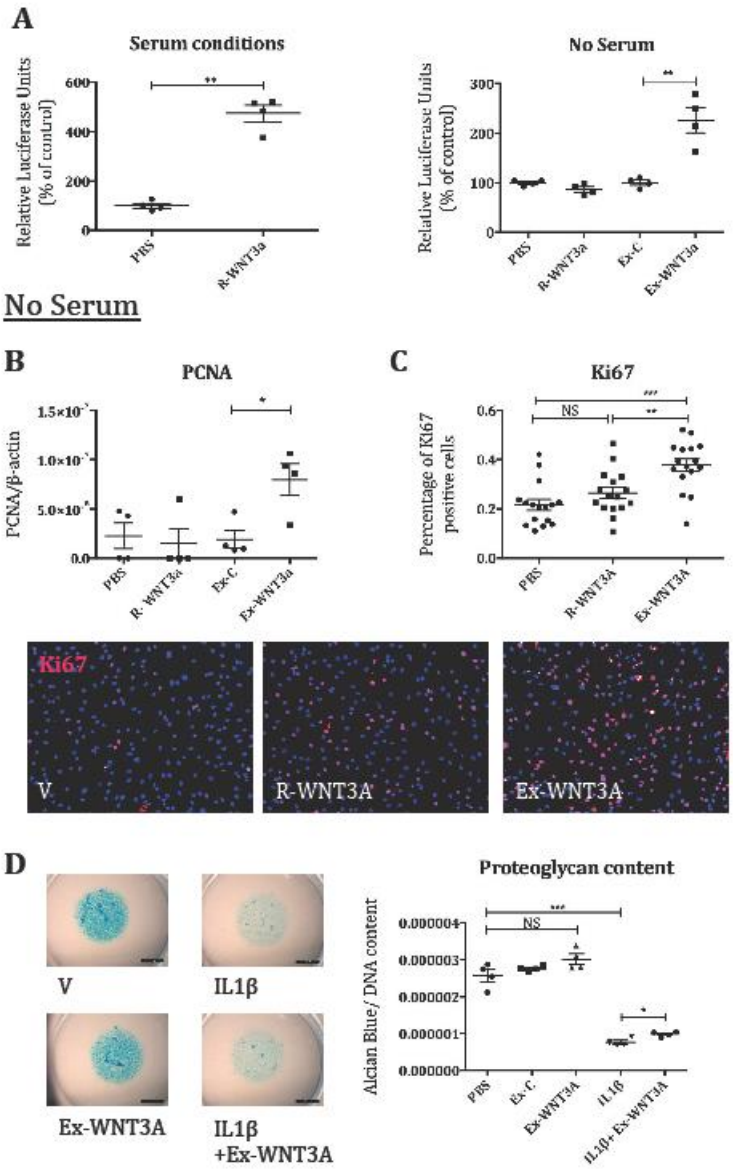
A
Serum conditions
Relative Luciferase Units (% of control)
PBS
R-WNT3a
No Serum
Ex-C
Ex-WNT3a
No Serum
B
PCNA
PCNA/β-actin
C
Ki67
Percentage of Ki67 positive cells
NS
PBS
R-WNT3A
Ex-WNT3A
Ki67
V
R-WNT3A
Ex-WNT3A
D
V
IL1β
Ex-WNT3A
IL1β +Ex-WNT3A
Proteoglycan content
Alcian Blue/ DNA content
Ex-C
IL1β
IL1β+Ex-WNT3A

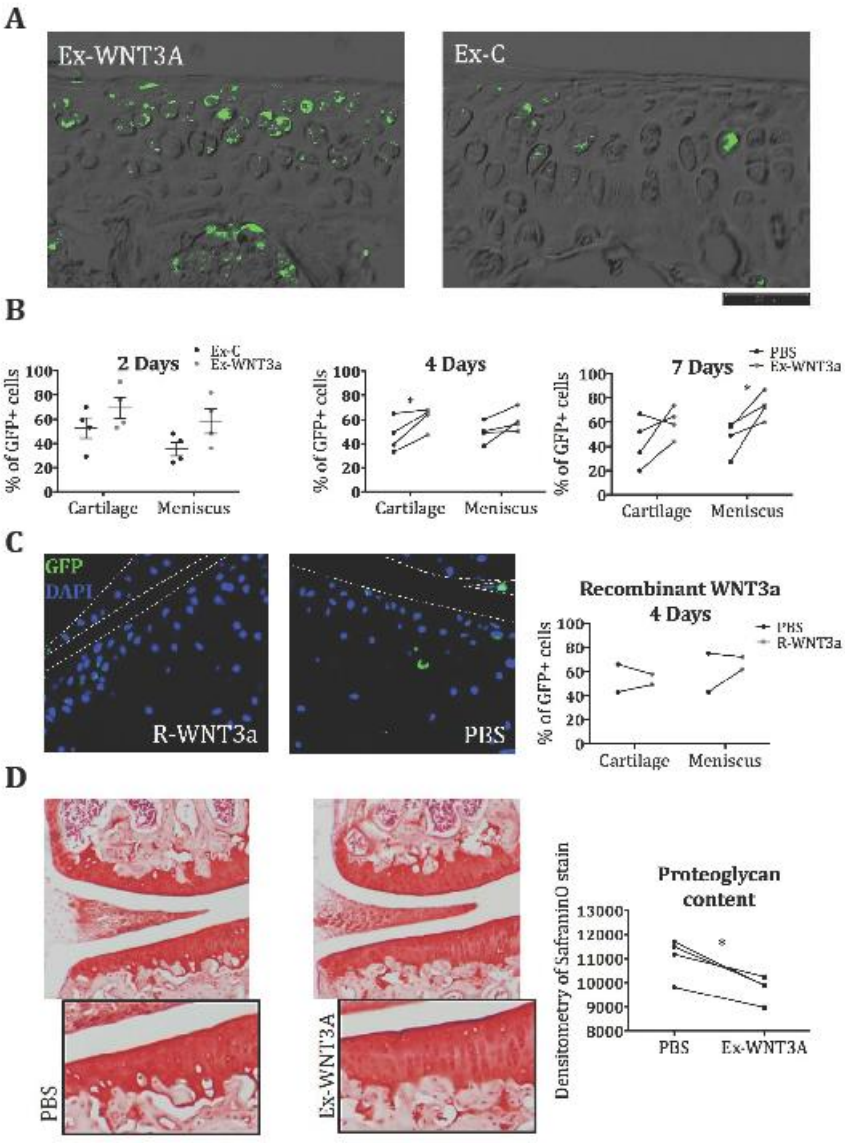
A
Ex-WNT3A
Ex-C
B
2 Days
4 Days
7 Days
Ex-C
Ex-WNT3a
PBS
Ex-WNT3a
% of GFP+ cells
100
80
60
40
20
0
Cartilage
Meniscus
C
GFP
DAPI
R-WNT3a
PBS
Recombinant WNT3a
4 Days
PBS
R-WNT3a
% of GFP+ cells
Cartilage
Meniscus
D
PBS
Ex-WNT3A
Densitometry of SafraninO stain
Proteoglycan
content
13000
12000
11000
10000
9000
8000
*
PBS
Ex-WNT3A

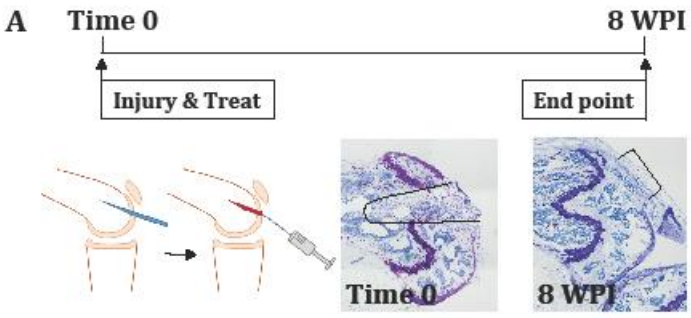
A
Time 0
8 WPI
Injury & Treat
End point
Time 0
8 WPI

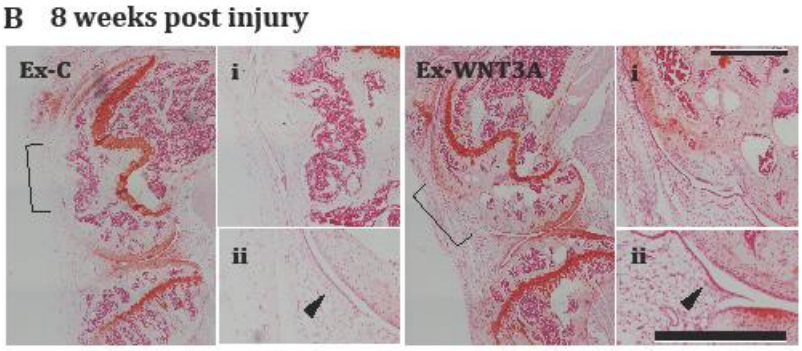
B 8 weeks post injury
Ex-C
i
ii
Ex-WNT3A
i
ii

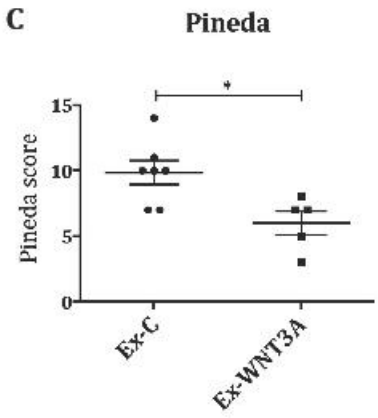
C
Pineda
*
Pineda score
15
10
5
0
Ex-C
Ex-WNT3A

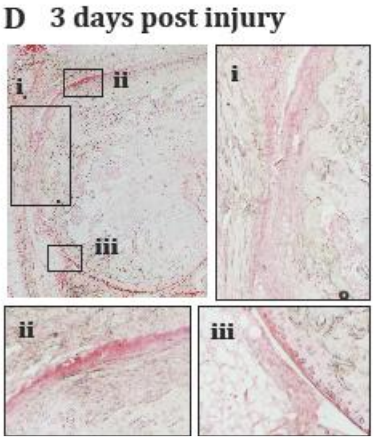
D 3 days post injury
i
ii
iii
i
ii
iii

SUPPLEMENTARY MATERIAL

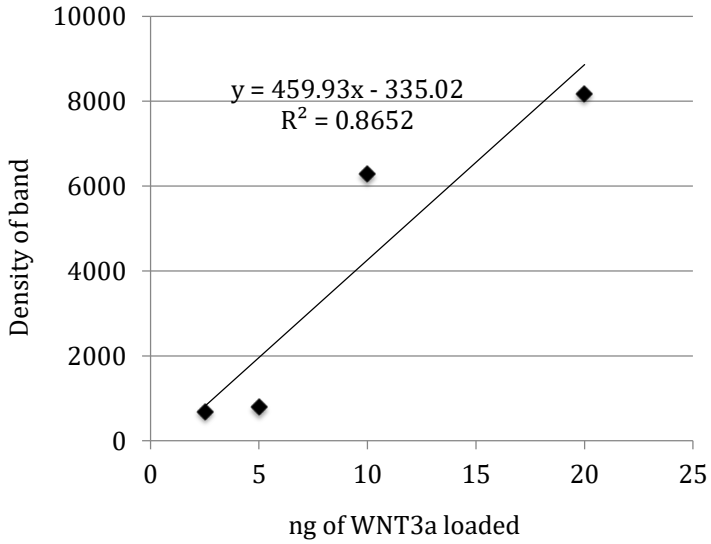

Volume Exosome preparation loaded	Conversion to ng using standard curve	ng/µl
20ul	125.05	6.25
10ul	94.60	9.46
5ul	37.56	7.51
2.5ul	15.64	6.25

Average ng/µl	7.4 (+/- 1.51)
Particle concentration	1700000/µl
ng of WNT3a per particle	4.34E-06

0.00434 pg of wnt3a per particle

Supplementary figure 1: To calculate the concentration of WNT3a in the exosomes, different concentrations of R-WNT3a were run on a western blot and the band density was calculated to generate a standard curve. On the same blot, Ex-WNT3a was also run and the concentrations extrapolated using the standard curve. Three different exposures were generated for the blot and the most appropriate was selected for concentration analysis. Variance is represented as +/- standard deviation.